International Journal of Biological Macromolecules 113 (2018) 558–564

Contents lists available at ScienceDirect

International Journal of Biological Macromolecules

journal homepage: https://www.journals.elsevier.com/ijbiomac

Structure and conformation of α-glucan extracted from *Agaricus blazei* Murill by high-speed shearing homogenization

Anqiang Zhang [a,*], Jiaying Deng [a], Xiaoqing Liu [a], Pengfei He [a], Liang He [b], Fuming Zhang [c], Robert J. Linhardt [c,d], Peilong Sun [a]

[a] Department of Food and Technology, Zhejiang University of Technology, Hangzhou, Zhejiang 310014, PR China
[b] The Key Laboratory of Biological and Chemical Utilization of Zhejiang Province, Zhejiang Forestry Academy, Hangzhou 310023, China
[c] Department of Chemical and Biological Engineering, Center for Biotechnology and Interdisciplinary Studies, Rensselaer Polytechnic Institute, Troy, NY 12180, USA
[d] Departments of Chemistry and Chemical Biology and Biomedical Engineering, Department of Biological Science, Center for Biotechnology and Interdisciplinary Studies, Rensselaer Polytechnic Institute, Troy, NY 12180, USA

ARTICLE INFO

Article history:
Received 4 January 2018
Received in revised form 23 February 2018
Accepted 24 February 2018
Available online 01 March 2018

Keywords:
Agaricus blazei Murill
Polysaccharide
Structure
Chain conformation
High-speed shearing homogenization

ABSTRACT

Agaricus blazei Murill is an edible and medicinal mushroom favored in many countries, by virtue of both its delicious taste and its potential health benefits such as its purported anticancer activity. A neutral α-glucan (ABM40-1) with a carbohydrate content of 96% was purified from the high-speed shearing homogenization extracts of *A. Blazei* Murill by ethanol precipitation and column chromatography. Methylation analysis along with nuclear magnetic resonance spectroscopy revealed that ABM40-1 was an α-(1 → 4)-D-glucopyranan with *O*-6 position occasionally occupied with α-Glc*p*-(1 → or α-Glc*p*-(1 → 6)-β-Glc*p*-(1 → side chains. A weight-average molecular weight of 7.34×10^6 Da was determined for ABM40-1 and its chain in solution was revealed as a compact sphere by size exclusion chromatography (SEC) coupled with a laser light scattering. This spherical conformation was also further confirmed by Congo red test and using atom force microscopy. These results suggest it would be worthwhile to further study the potential bioactivities of ABM40-1.

1. Introduction

Agaricus blazei Murill, also known as *Himematsutake* in Japan and *Jisongrong* in China, is an edible and medicinal mushroom native to Brazil. It is widely cultivated and consumed in countries including Japan and China based on demands for it as a food and also for its potential health benefits. A wide range of biological functions has been reported for this mushroom, including anticancer, anti-mutagenicity, chemopreventive, antioxidant activities [1–4]. Among the components determining these functions of *A. Blazei* Murill are polysaccharides, which are believed to significantly contribute to the anticancer, antioxidation and immunomodulating bioactivities of *A. Blazei* Murill [5–7]. The structural characteristics of polysaccharides from *A. Blazei* Murill have also attracted increasing attention because of their vital roles in the activities, for example, the structure of β-D-glucans isolated from *A. Blazei* Murill have been reported [8,9].

Hot water extraction is the most common technique for the preparation of polysaccharides, but it is generally of low efficiency, time-consuming and energy-intensive. Some alternative extraction methods have been developed, such as ultrasonic-assisted and enzyme-assisted extraction [10,11]. High-speed shearing homogenization extraction, an emerging novel method to extract bioactive ingredients, has also been successfully used for the high efficiency extraction of polysaccharides like pectin [12].

The present study focuses on the extraction of a homogenous glucan isolated from *A. Blazei* Murill using high-speed shearing homogenization. The detailed structural features of this glucan were determined using chemical analysis and NMR spectroscopy. A determination of the solution conformation of this glucan was also performed since its conformation impacts its activities.

2. Materials and methods

2.1. Materials

The fruiting bodies of *A. blazei* Murill were provided by Hangzhou Baishanzu Biological Technology Co., Ltd., China and identified by Prof. Weiming Cai, Zhejiang Forestry Academy.

Diethylaminoethyl (DEAE) Sepharose fast flow and Sephacryl S-500 high-resolution were purchased from GE Healthcare. Monosaccharide standards (L-Rha, L-Fuc, L-Ara, D-Xyl, D-Man, D-Glc, D-Gal), dimethyl sulfoxide (DMSO), methyl iodide (CH_3I), sodium borohydride ($NaBH_4$), trifluoroacetic acid (TFA) and Congo red were obtained from Sigma.

* Corresponding author.
E-mail address: zhanganqiang@zjut.edu.cn (A. Zhang).

https://doi.org/10.1016/j.ijbiomac.2018.02.151
0141-8130/

All other reagents and solvents were of analytical grade and made in China.

2.2. Isolation and purification of polysaccharide

The fruiting bodies of *A. blazei* Murill were ground and then soaked overnight with 95% ethanol to remove ethanol extractable molecules. After removing alcohol by filtration, the residues were extracted with distilled water through a high-speed shearing homogenization technique at room temperature. The aqueous extracts were pooled and concentrated under reduced pressure. Furthermore, removing protein using Sevag method was repeatedly performed six times for the concentrate, followed by ethanol precipitation by slowly adding ethanol to a final concentration of 40 vol%. The resulting crude polysaccharide fraction (sediments) was collected, lyophilized, and designated as ABM40.

ABM40 was dissolved in distilled water and then subjected to the DEAE Sepharose column (26 mm × 100 cm) chromatography with step-wise salt elution (0, 0.1, 0.2 M). Additional purification of the fraction eluting at salt concentration of 0.1 M was performed by chromatography on Sephacryl S-500 column (16 mm × 100 cm) eluted with water. Elution was monitored by determining sugar content in the eluent by phenol sulfuric acid method [13]. The main polysaccharide fractions were pooled, lyophilized, and designated as ABM40-1.

2.3. Physicochemical properties

The ultraviolet (UV) scan of ABM40-1 from 400 to 200 nm was conducted using a UV-2450 scanning ultraviolet/visible (UV/Vis) spectrophotometer (Shimadzu Co., Japan).

Fourier transform infrared (FT–IR) spectroscopy of ABM40-1 was recorded using KBr pellets on a Nicolet 6700 FT–IR spectrometer (Thermo, USA) in the range between 4000 and 500 cm^{-1}.

2.4. Monosaccharide compositional analysis

Acetylation was performed before gas chromatography–mass spectrometry (GC–MS) analysis of monosaccharide compositions of ABM40-1 as described in our previous report [14]. Briefly, 2 mg of ABM40-1 was hydrolyzed with TFA (2 M, 4 mL) at 110 °C for 2 h, followed by rotary evaporation to remove excess TFA with methanol. The released monosaccharides were reduced through addition of $NaBH_4$ solution (10 mg/mL, 3 mL) for 3 h and then acetylated with acetic anhydride (4 mL) at 100 °C for 1 h. The resulting alditol acetates were determined by GC–MS equipped with an HP–5MS capillary column (30 m × 0.32 mm × 0.25 μm). The oven temperature program was set: 120 °C (holding for 1 min) to 165 °C (for 1 min) at 10 °C/min, to 169 °C (for 0.5 min) at 1 °C/min, to 196 °C (for 0.5 min) at 10 °C/min, to 200 °C (for 1 min) at 1 °C/min, to 240 °C (for 5 min) at 10 °C/min. The temperatures of both injector and detector were set at 250 °C. Helium was used as carrier gas. For qualitative analysis of monosaccharides in ABM40-1, monosaccharide standards were subjected to the same treatments of reduction and acetylation as above.

2.5. Methylation analysis

ABM40-1 was converted into partially methylated alditol acetates (PMAAs) as described by Anumula and Taylor [15]. Briefly, 3 mg of ABM40-1 was dissolved in DMSO (0.6 mL), followed by addition of a fine slurry of NaOH in DMSO (0.6 mL) and methyl iodide (0.6 mL). After incubating for 10 min, distilled water was added to terminate the methylation reaction and $CHCl_3$ was then added to extract the resulting products. For complete methylation this procedure was repeated again on the $CHCl_3$ extract after evaporation resulting in the disappearance of the hydroxyl absorption in IR spectrum. The permethylated polysaccharide was successively hydrolyzed with HCO_2H (88%, 3 mL) at 100 °C for 3 h and TFA (2 M, 4 mL) at 110 °C for 6 h. Reduction and acetylation of the hydrolysate were then performed as described in the monosaccharide analysis. The generated PMAAs were recovered by extraction with $CHCl_3$ and determined by GC–MS. The oven temperature was programmed as follows: initial temperature of 120 °C after holding 1 min were elevated to 240 °C at 10 °C/min and keeping constant for 6.5 min. The other parameters of GC–MS were set as described in the monosaccharide analysis.

2.6. NMR analysis

ABM40-1 (30 mg) was thrice deuterium exchanged by freeze-drying from D_2O before dissolution in D_2O (0.5 mL) for NMR analysis on a Bruker AVANCE III (500 MHz) NMR spectrometer. The NMR spectra were recorded including ^1H–(25 °C and 60 °C) and ^{13}C NMR, ^1H–^1H correlation spectroscopy (COSY), total correlation spectroscopy (TOCSY), nuclear Overhauser enhancement spectroscopy (NOESY), heteronuclear single-quantum correlation (HSQC), heteronuclear multiple bond correlation (HMBC). ^1H and ^{13}C chemical shifts were calibrated through δ 4.78 for HOD (25 °C) and δ 0.00 for 4,4-dimethyl-4-silapentane-1-sulfonic acid (DSS), respectively.

2.7. Congo red test

An aliquot of ABM40-1 aqueous solution (2 mL) was mixed with the same volume of Congo red (80 μM) aqueous solution. NaOH solution (1 M) and water were also added into the mixture to bring the final NaOH concentrations to 0, 0.05, 0.10, 0.15, 0.20, 0.25, 0.30, 0.35, 0.40, 0.45, 0.50 M. Water was used in place of ABM40-1 as negative control. The maximum absorbance wavelength (λ_{max}) in the range from 400 to 600 nm was measured using a scanning ultraviolet/visible spectrometer.

2.8. SEC-MALLS-RI

Molecular weight and conformation parameters in solution of ABM40-1 were determined using size exclusion chromatography (SEC) equipped with a multi-angle light scatter detector and a refractive index detector (SEC-MALLS-RI). This determination was performed on TSK-Gel G5000 PW_{XL} and TSK-Gel G3000 PW_{XL} columns coupled in series. $NaNO_3$ solution (1.0 M) containing 0.05% (w/w) NaN_3 was used at a flow rate of 1.0 mL/min for elution. ABM40-1 solution (3.0 mg/mL) was prepared by completely dissolving sample in mobile phase and filtered through a 0.45-μm filter before injection on the column. The refractive index increment value (dn/dc) of 0.138 mL/g was adopted in this study. ASTRA software was used to acquire and analyze the experimental data.

2.9. Atomic force microscopy

ABM40-1 was dissolved in Milli-Q water and stirred for 4 h at 80 °C to yield a 1.0 mg/mL stock solution. The test sample solution was prepared by dilution of the stock solution into 5 μg/mL with Milli-Q water and stirred for 2 h at 80 °C before deposition on cleaved mica. After adsorption for 30 s at RT, the sample on mica was thoroughly rinsed with 1.0 mL Milli-Q water and dried in air for Atomic force microscopy (AFM) imaging. AFM was operated on a Park XE-70 Atomic Force Microscope (Park Scientific Instruments, Korea) and in tapping mode under ambient conditions using commercial silicon nitride cantilevers. While flattening was used to remove background curvature, no further image processing was carried out on the AFM images.

3. Results and discussion

3.1. Preparation and physicochemical properties of ABM40-1

Isolated of extracts of fruiting bodies of *A. blazei* using high-speed shearing homogenization and chromatography on a DEAE-Sepharose

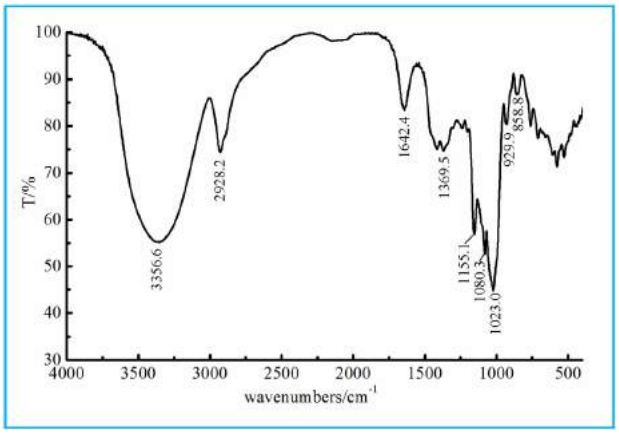

Fig. 1. IR spectrum of ABM40-1 isolated from *A. Blazei* Murill.

column and a Sephacryl S-500 column and ethanol precipitation (final alcohol concentration of 40 vol%) afforded a polysaccharide termed ABM40-1. The carbohydrate content of ABM40-1 was 96% as determined by phenol sulfuric acid method (Dubois et al., 1956) using glucose as the standard. Absence of absorption at 280 nm in UV scanning spectrum demonstrated that no protein was present in ABM40-1.

The FT-IR spectrum (Fig. 1) of ABM40–1 showed the characteristic absorptions of a polysaccharide. An O—H stretching vibration was indicated by an intense broad peak at 3356.6 cm^{-1}. A C—H stretching vibration band at 2928.2 cm^{-1} and bending vibration peaks at ~1369.5 cm^{-1} were observed. Stretching vibrations of C—O—C and C—O—H contributed the absorption peaks in the range from 1000 to 1200 cm^{-1}. Furthermore, the peak at 1642.4 cm^{-1} was ascribed to associated water. The absorption band at 858.8 cm^{-1} suggested that ABM40-1 contained the sugar moieties with α-anomeric configurations. An absorption band at ~1730.0 cm^{-1} was not observed demonstrating ABM40-1 was free of uronic acids.

3.2. Structural analysis of ABM40-1

3.2.1. Monosaccharide compositions

The acetate derivatives of glucose were the only product generated from ABM40-1 in monosaccharide compositional analysis, suggesting that ABM40-1 was a glucan.

3.2.2. Methylation analysis

Methylation analysis had been extensively used in structure analysis of polysaccharides as a typical technique for elucidation of the types of glycosyl linkages. ABM40-1 was next subjected to methylation analysis to determine the types of glycosyl linkages present. GC–MS revealed four PMAAs, which were identified by their major mass fragments as 2,3,4.6-tetra-*O*-methyl-glucose, 2,3,6-tri-*O*-methyl-glucose, 2,3,4-tri-*O*-methyl-glucose and 2,3-di-*O*-methyl-glucose (Table 1). Thus, ABM40-1 is mainly comprised of non-reducing terminal, 4-linked, 6-linked and 4,6-linked glucose residues. From the integration of the corresponding peaks, the ratio of these linkages was calculated to be approximately 1.0:7.36:0.27:0.78. The 4,6-linkage demonstrates that ABM40-1 is a branched polysaccharide. The branching degree (DB) was ~19% based on the following equation [16]:

$$\mathrm{DB} = \frac{N_B + N_T}{N_B + N_T + N_L}$$

where, N_B, N_T and N_L are the total numbers of the terminal residues, branched residues, and linear residues, respectively.

3.2.3. NMR analysis

NMR spectroscopy was used to further establish the extract structure and conformation of ABM40-1. In addition to an anomeric signal at about δ 5.41, the ^{1}H NMR spectrum (25 °C) of ABM40-1 shows three weak signals at δ 5.24, 4.66 and 4.54 in the anomeric region (δ 4.30–5.90). The ^{1}H NMR spectrum recorded at 60 °C demonstrated that no additional anomeric proton signals were under the HOD peak at δ 4.78 in the ^{1}H NMR spectrum acquired at 25 °C. Non-anomeric protons could be found in the range between δ 3.20 and 4.27. In the ^{13}C and DEPT−135 NMR spectrum, four anomeric carbon signals were clearly observed at δ 102.98, 100.05, 99.73 and 99.60. Furthermore, another two anomeric carbon signals at δ 92.00 and 95.89 were also assigned from the HSQC spectrum (Fig. 2a). The other carbon signals fell in the range of δ 60.00 to 80.00. The negative peaks arising from methylene in DEPT-135 NMR spectrum at δ 68.97, 62.54, 60.48 and 60.43 were assigned to the C6 of hexoses. As indicated in HSQC spectrum, the proton signal at δ 5.41 included anomeric protons of three residues with anomeric carbon signals at δ 100.05, 99.73 and 99.60. Three additional anomeric protons, at δ 5.24, 4.66 and 4.54, were observed in ABM40-1 and are denoted as A to F (Table 2).

2D NMR spectra were employed to assign the chemical shifts to identify the residues present. Starting from the anomeric protons, the chemical shifts of other protons were assigned by tracing correlation resonances in COSY spectrum (Fig. 2b) and these assignments were confirmed based on resonances in TOCSY and NOESY spectra. The HSQC spectrum gave the information on the chemical shifts of carbons. All chemical shifts are summarized in Table 2 and these were used to identify the saccharide residues.

The identification of magnetization transfer from H1 to H5 in TOCSY revealed that these residues had a *gluco*-configuration, agreeing well with the results of the monosaccharide compositional analysis. The α-configurations of residues A through D were confirmed from the chemical shifts of anomeric protons being >4.90 δ and their coupling constants ($J_{1,2}$) being <4 Hz. The β-configurations of residues E and F were confirmed by their anomeric proton resonances occurring in the region from δ 4.40 to 4.80 and their coupling constants ($J_{1,2}$) of ~8 Hz. The identification of linkage positions was determined based on the downfield shift of linkage carbons signals compared to analogous reference compounds. For example, the downfield shift of C4 revealed that residue A was a →4)-α-Glc*p*-(1→. Similarly, residue B to F were identified as α-Glc*p*-(1→, →4,6)-α-Glc*p*-(1→, →4)-α-Glc*p*, →4)-β-Glc*p* and →6)-β-Glc*p*-(1→, respectively.

NOESY and HMBC spectra were employed for determination of the sequences of these residues. The NOE resonance at $\delta_{H/H}$ 5.41/3.66 reveals that residue A was linked by itself or residue C through (1 → 4) linkages and this was also confirmed by the long-range correlations in

Table 1
The results of methylation analysis of ABM40-1

Retention time (min)	Methylated sugars	Substituted sugar unit	Molar ratios	Major mass fragments (*m*/*z*)
9.57	2,3,4,6-Me_4-Glc*p*[a]	T-linked Glc*p*	1	43, 71, 87, 101, 117, 129, 145, 161, 205
10.62	2,3,6-Me_3-Glc*p*	1,4-linked Glc*p*	7.36	43, 87, 101, 113, 117, 129, 143, 161, 173, 233
10.84	2,3,4-Me_3-Glc*p*	1,6-linked Glc*p*	0.27	43, 71, 87, 101, 117, 129, 161, 173, 189, 233
11.69	2,3-Me_2-Glc*p*	1,4,6-linked Glc*p*	0.78	43, 85, 101. 117, 127, 159, 187, 201, 261

[a] 2,3,4,6-Me_4-Glc*p* is the abbreviation of 1,5-di-*O*-acetyl-2,3,4,6-tetra-*O*-methyl-glucose, *p* means pyranose.

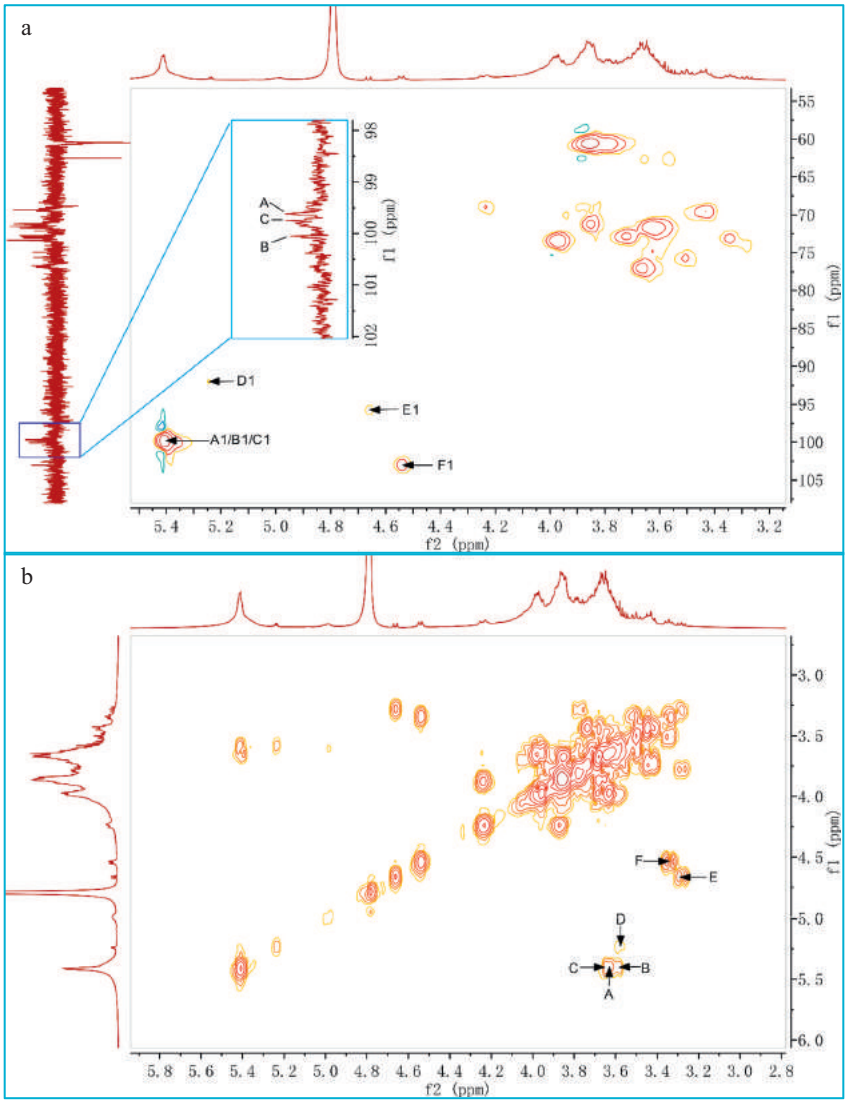

Fig. 2. Two-dimensional NMR spectra of ABM40-1 isolated from *A. Blazei* Murill. (a), HSQC spectrum; (b), $^{1}H - {}^{1}H$ COSY spectrum. The letters A to F represent the six residues of ABM40-1 shown in Table 2.

HMBC spectrum at $\delta_{H/C}$ 5.41/77.09 and $\delta_{H/C}$ 3.66/99.60. The NOE resonance at $\delta_{H/H}$ 4.54/3.87 and the HMBC resonances at $\delta_{H/C}$ 4.54/77.09 and $\delta_{H/C}$ 3.87/102.98, demonstrate the connection of residue F to the *O*-6 of residue C through (1 → 6) linkages. Residue F is terminated by non-reducing terminal residue B. Moreover, portion of residue B also links directly to the *O*-6 of residue C, based on a significantly larger amount of residue C than residue F, which was demonstrated by methylation analysis (Table 1). Residue D and E were at the reducing terminus of the main chain.

Table 2
^{1}H and ^{13}C chemical shifts data (ppm) of ABM40-1

Residues	H1/C1	H2/C2	H3/C3	H4/C4	H5/C5	H6a, 6b/C6
→4)-α-Glc*p*-(1→	5.41	3.63	3.97	3.66	3.85	3.78, 3.86
A	99.60	71.76	73.41	77.09	71.26	60.43
α-Glc*p*-(1→	5.41	3.59	3.73	3.43	3.68	3.78, 3.86
B	100.05	71.76	73.06	69.65	72.19	60.43
→4,6)-α-Glc*p*-(1→	5.41	3.65	3.97	3.68	3.94	3.87, 4.24
C	99.73	71.85	73.41	77.09	70.21	68.97
→4)-α-Glc*p*	5.24	3.58	3.98	3.63	3.94	3.80, 3.87
D	92.00	71.76	73.41	77.66	70.21	60.48
→4)-β-Glc*p*	4.66	3.28	3.77	3.63	3.60	3.56, 3.65
E	95.89	74.12	76.18	77.09	74.33	62.54
→6)-β-Glc*p*-(1→	4.54	3.34	3.50	3.47	3.64	3.85, 4.24
F	102.98	73.13	75.70	69.75	74.87	68.97

Methylation and NMR analyses demonstrate that ABM40–1 has a main chain of α-(1 → 4)-D-glucopyranan, which was partially substituted at *O*-6 position by α-Glc*p*-(1 → or α-Glc*p*-(1 → 6)-β-Glc*p*-(1→. The proposed structure in of the ABM40–1 repeating unit contains a reducing terminal →4)-α-Glc*p* and →4)-β-Glc*p* (Fig. 3). A similar structure was reported for α-glucan from *Coprinus comatus* [17].

3.3. Congo red test

A Congo red-glucan complex generally forms when Congo red is mixed under alkaline conditions with a glucan having a triple-helical conformation, leading to an increased absorption maxima wavelength (λ_{max}). This phenomenon has been successfully used to identify the triple-helical conformation of glucans, such as polysaccharide (JQPs)

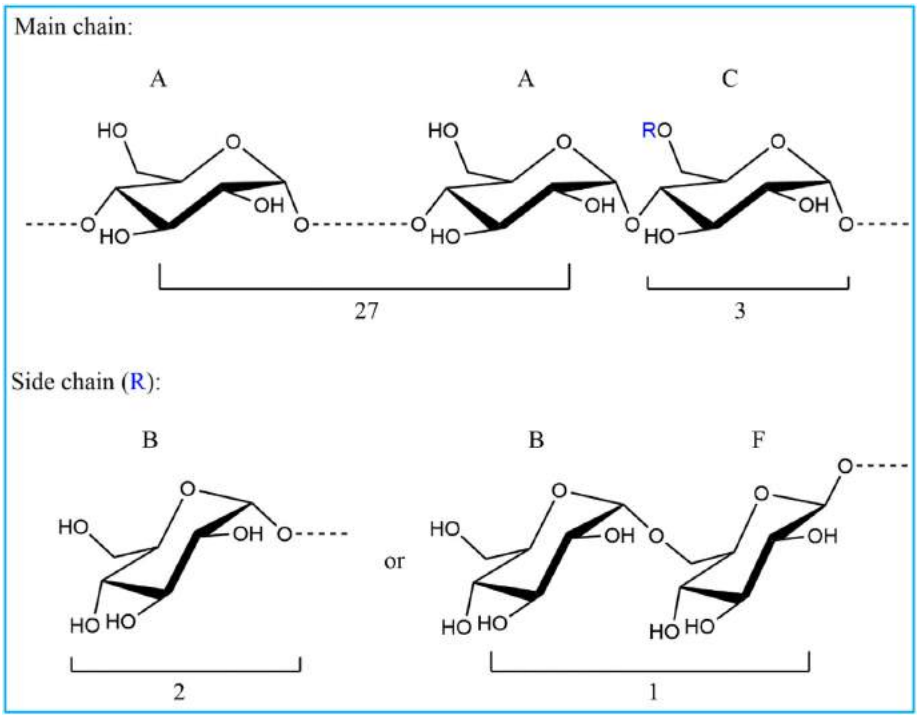

Fig. 3. The proposed structure for the repeating unit of ABM40-1 isolated from *A. Blazei* Murill.

isolated from Jiqian mushroom [18]. However, the polysaccharide with a flexible random coil chain isolated from *Bacillus Calmette* Guerin formulation [19] showed no significant red shift in its λ_{max} using a Congo red test (Fig. 4a), suggesting that ABM40–1 did not exhibit a triple-helical conformation at alkali concentrations of 0 to 0.5 mol/L.

3.4. SEC-MALLS-RI

The combination of size exclusion chromatography with multi-angle laser light scattering (SEC-MALLS) analysis has been increasingly used in determining the conformation of polysaccharides [20–22]. SEC-

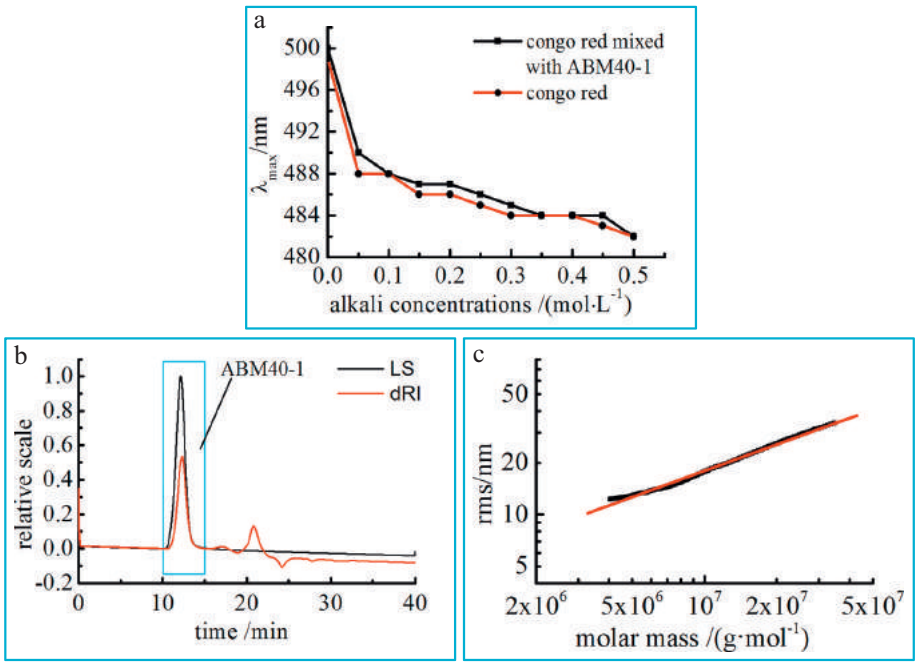

Fig. 4. (a), The changes of λ_{max} with concentrations of NaOH in Congo red test; (b), The SEC chromatogram of ABM40-1 with the MALLS and the RI detectors; (c), The log-log plot of radius of gyration versus molecular weight for ABM40-1 isolated from *A. Blazei* Murill. (For interpretation of the references to color in this figure legend, the reader is referred to the web version of this article.)

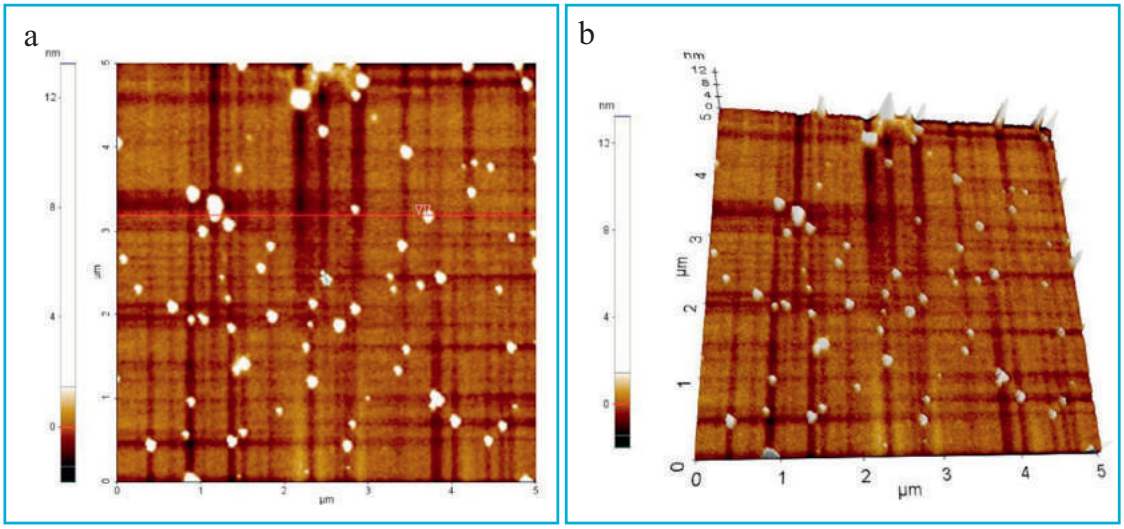

Fig. 5. AFM images of ABM40-1 isolated from *A. Blazei* Murill, (a), planar image; (b), three-dimensional image.

MALLS generates molecular information, molecular weights and radius of gyration ($\langle S^2\rangle 1/2$ z), and also affords a power exponent ν, arising from the equation $\langle S^2\rangle_z^{1/2} = kM_w^{\nu}$. The ν value can be used to elucidate the conformation of polysaccharides in solution, with a value of ~0.3 generally corresponding to sphere-like chains, 0.5–0.6 corresponding to flexible chains in a good solvent, and 0.7–1.0 corresponding to semi-flexible chains [23,24].

The SEC chromatograms, recorded with both MALLS and RI detectors (Fig. 4b), revealed a single symmetrical peak, implying ABM40-1 is a relatively homogeneous polysaccharide. The second weak RI peak was a system peak. By computing a typical Zimm plot from the light scattering data at different angles for each concentration obtained from the RI data, the molecular parameters of ABM40-1 were determined as: weight-average molecular weight (M_w) of 7.34×10^6 Da, number-average molecular weight (M_n) of 5.53×10^6 Da, *z*-average molecular weight (M_z) of 1.14×10^7 Da and $\langle S^2\rangle 1/2$ z of 19.4 nm. The low polydispersity index (PDI) was calculated as 1.33 from the ratio of M_w to M_n, suggesting the narrow molecular mass distribution for ABM40-1. Meanwhile, a ν value of 0.29 was determined from the slope of double logarithmic plot of $\langle S^2\rangle 1/2$ z against M_w (Fig. 4c). The ν value around 0.3 indicated a sphere-like conformation in solution for ABM40-1, which corroborated the results in Congo red test.

3.5. Molecular morphology

AFM has been a powerful technique to directly observe the conformation of polysaccharide chain in the natural environments from which they originated [25]. Spherical particles could be clearly observed in the planar and three-dimensional AFM images of ABM40-1 (Fig. 5), demonstrating the spherical conformation for ABM40-1 at a concentration of 5 μg/mL. It is preferable to characterize the molecule size by height measurement of AFM images because of the large overestimation of width measurement arising from the tip broadening effects [26]. The heights of spherical particles in Fig. 5 in the range of 3–8 nm, significantly larger than average heights of a single polysaccharide chain ranging from 0.1 to 1 nm [27], suggesting that the molecular chains of ABM40–1 may entangle or aggregate with each other to present a spherical chain conformation in aqueous solution. These results on the molecular morphology of ABM40-1 were in good agreement with those obtained using SEC-MALLS-RI.

Taking all the above results together, the structure and conformation of ABM40-1 was in similar to those of the polysaccharide (BDP) purified from *Bacillus Calmette* Guerin formulation, which is a branched α-(1 → 4)-linked D-glucopyranan with a globular like chain structure in solution [19]. The BDP polysaccharide was also reported to exhibit significant immunomodulatory activity. ABM40-1 may also display immunomodulatory activity since structure and conformation play a vital role on activity. Additional experiments should concentrate on the potential important bioactivities of ABM40-1 and the relationship between its structural features and biological functions.

4. Conclusion

After extraction of the fruiting bodies of *A. Blazei* Murill by high-speed shearing homogenization, a homogeneous polysaccharide denoted as ABM40-1 was obtained from the extract through a series of purification procedures. ABM40-1 is a water-soluble branched glucan with a high carbohydrate content of 96% and a low branching degree of 19%. Its backbone comprised of →4)-α-Glc*p*-(1→ and is occasionally substituted at *O*-6 positions with side chains of α-Glc*p*-(1→ or α-Glc*p*-(1 → 6)-β-Glc*p*-(1→. The reducing terminal, terminating the backbone structure, is →4)-α-Glc*p* or →4)-β-Glc*p*. ABM40-1 had a low polydispersity index of 1.33 and a M_W of 7.34×10^6 Da and an M_n of 5.53×10^6 Da. In solution ABM40-1 has a spherical conformation, as determined by SEC-MALLS-RI, Congo red test and using AFM. Further work aimed at studying the bioactivities of ABM40-1 is planned in the future.

Acknowledgements

The study was supported by the National Natural Science Foundation of China (Grant No. 31671813) and Natural Science Foundation of Zhejiang Province (Grant No. LY17C200017).

References

[1] H. Akiyama, M. Endo, T. Matsui, I. Katsuda, N. Emi, Y. Kawamoto, T. Koike, H. Beppu, Agaritine from *Agaricus blazei* Murrill induces apoptosis in the leukemic cell line U937, Biochim. Biophys. Acta 1810 (2011) 519–525.
[2] Z.R. Guterrez, M.S. Mantovani, A.F. Eira, L.R. Ribeiro, B.Q. Jordão, Variation of the antimutagenicity effects of water extracts of *Agaricus blazei* Murrill in vitro, Toxicol. in Vitro 18 (2004) 301–309.
[3] S. Jia, F. Li, Y. Liu, H. Ren, G. Gong, Y. Wang, S. Wu, Effects of extraction methods on the antioxidant activities of polysaccharides from *Agaricus blazei* Murrill, Int. J. Biol. Macromol. 62 (2013) 66–69.
[4] F. Pinheiro, R.R. Faria, J.L.V.D. Camargo, A.L.T. Spinardi-Barbisan, A.F.D. Eira, L.F. Barbisan, Chemoprevention of preneoplastic liver foci development by dietary mushroom *Agaricus blazei* Murrill in the rat, Food Chem. Toxicol. 41 (2003) 1543–1550.

[5] M. Kozarski, A. Klaus, M. Niksic, D. Jakovljevic, J.P.F.G. Helsper, L.J.L.D. Van Griensven, Antioxidative and immunomodulating activities of polysaccharide extracts of the medicinal mushrooms *Agaricus bisporus*, *Agaricus brasiliensis*, *Ganoderma lucidum* and *Phellinus linteus*, Food Chem. 129 (2011) 1667–1675.
[6] S. Wu, F. Li, S. Jia, H. Ren, G. Gong, Y. Wang, Z. Lv, Y. Liu, Drying effects on the antioxidant properties of polysaccharides obtained from *Agaricus blazei* Murrill, Carbohydr. Polym. 103C (2014) 414–417.
[7] L. Yue, H. Cui, C. Li, Y. Lin, Y. Sun, Y. Niu, X. Wen, J. Liu, A polysaccharide from *Agaricus blazei* attenuates tumor cell adhesion via inhibiting E-selectin expression, Carbohydr. Polym. 88 (2012) 1326–1333.
[8] Q. Dong, J. Yao, X.T. Yang, J.N. Fang, Structural characterization of a water-soluble beta-D-glucan from fruiting bodies of *Agaricus blazei* Murr, Carbohydr. Res. 337 (2002) 1417–1421.
[9] M.L.C. Gonzaga, T.M.F. Menezes, J.R.R. de Souza, N.M.P.S. Ricardo, S.d.A. Soares, Structural characterization of β glucans isolated from *Agaricus blazei* Murill using NMR and FTIR spectroscopy, Bioact. Carbohydr. Diet. Fibre 2 (2013) 152–156.
[10] S. Wang, X. Dong, J. Tong, Optimization of enzyme-assisted extraction of polysaccharides from alfalfa and its antioxidant activity, Int. J. Biol. Macromol. 62 (2013) 387–396.
[11] Y. Zheng, Y. Li, W.d. Wang, Optimization of ultrasonic-assisted extraction and in vitro antioxidant activities of polysaccharides from *Trametes orientalis*, Carbohydr. Polym. 111 (2014) 315–323.
[12] X. Guo, W. Zhao, X. Pang, X. Liao, X. Hu, J. Wu, Emulsion stabilizing properties of pectins extracted by high hydrostatic pressure, high-speed shearing homogenization and traditional thermal methods: a comparative study, Food Hydrocoll. 35 (2014) 217–225.
[13] M. Dubois, K.A. Gilles, J.K. Hamilton, P. Rebers, F. Smith, Colorimetric method for determination of sugars and related substances, Anal. Chem. 28 (1956) 350–356.
[14] P. He, A. Zhang, F. Zhang, R.J. Linhardt, P. Sun, Structure and bioactivity of a polysaccharide containing uronic acid from *Polyporus umbellatus* sclerotia, Carbohydr. Polym. 152 (2016) 222–230.
[15] K.R. Anumula, P.B. Taylor, A comprehensive procedure for preparation of partially methylated alditol acetates from glycoprotein carbohydrates, Anal. Biochem. 203 (1992) 101–108.
[16] L. Chen, J. Liu, Y. Zhang, B. Dai, Y. An, L.L. Yu, Structural, thermal, and anti-inflammatory properties of a novel pectic polysaccharide from Alfalfa (*Medicago sativa* L.) stem, J. Agric. Food Chem. 63 (2015) 3219–3228.
[17] B. Li, J.M. Dobruchowska, G.J. Gerwig, L. Dijkhuizen, J.P. Kamerling, Structural investigation of water-soluble polysaccharides extracted from the fruit bodies of *Coprinus comatus*, Carbohydr. Polym. 91 (2013) 314–321.
[18] Y. Liu, Y.Q. Du, J.H. Wang, X.Q. Zha, J.B. Zhang, Structural analysis and antioxidant activities of polysaccharide isolated from Jinqian mushroom, Int. J. Biol. Macromol. 64 (2014) 63–68.
[19] L. Wei, W. Hong, J. Yu, Y. Liu, W. Lu, C. Yin, L. Chao, C. Pan, W. Yao, X. Gao, Structure, chain conformation, and immunomodulatory activity of the polysaccharide purified from *Bacillus* Calmette Guerin formulation, Carbohydr. Polym. 150 (2016) 149–158.
[20] P.F. He, L. He, A.Q. Zhang, X.L. Wang, L. Qu, P.L. Sun, Structure and chain conformation of a neutral polysaccharide from sclerotia of *Polyporus umbellatus*, Carbohydr. Polym. 155 (2017) 61–67.
[21] S. Li, Y. Huang, S. Wang, X. Xu, L. Zhang, Determination of the triple helical chain conformation of β-glucan by facile and reliable triple-detector size exclusion chromatography, J. Phys. Chem. B 118 (2014) 668–675.
[22] D.T. Wu, L.Z. Meng, L.Y. Wang, G.P. Lv, K.L. Cheong, D.J. Hu, J. Guan, J. Zhao, S.P. Li, Chain conformation and immunomodulatory activity of a hyperbranched polysaccharide from *Cordyceps sinensis*, Carbohydr. Polym. 110 (2014) 405–414.
[23] J. Wang, Z. Ma, L. Zhang, Y. Fang, F. Jiang, G.O. Phillips, Structure and chain conformation of water-soluble heteropolysaccharides from *Ganoderma lucidum*, Carbohydr. Polym. 86 (2011) 844–851.
[24] L. Yang, L.M. Zhang, Chemical structural and chain conformational characterization of some bioactive polysaccharides isolated from natural sources, Carbohydr. Polym. 76 (2009) 349–361.
[25] K.P. Wang, J. Wang, Q. Li, Q.L. Zhang, R.X. You, Y. Cheng, L. Luo, Y. Zhang, Structural differences and conformational characterization of five bioactive polysaccharides from *Lentinus Edodes*, Food Res. Int. 62 (2014) 223–232.
[26] J. Wang, W. Yang, Y. Tang, Q. Xu, S. Huang, J. Yao, J. Zhang, Z. Lei, Regioselective sulfation of *Artemisia sphaerocephala* polysaccharide: solution conformation and antioxidant activities in vitro, Carbohydr. Polym. 136 (2016) 527–536.
[27] Y. Wang, Y. Peng, X. Wei, Z. Yang, J. Xiao, Z. Jin, Sulfation of tea polysaccharides: synthesis, characterization and hypoglycemic activity, Int. J. Biol. Macromol. 46 (2010) 270–274.